Pflugers Arch - Eur J Physiol (2016) 468:895–908
DOI 10.1007/s00424-015-1785-2

MOLECULAR AND CELLULAR MECHANISMS OF DISEASE

Adult nephron-specific MR-deficient mice develop a severe renal PHA-1 phenotype

Jérémie Canonica[1,2] · Chloé Sergi[1] · Marc Maillard[3] · Petra Klusonova[2,4] · Alex Odermatt[2,4] · Robert Koesters[5] · Dominique Loffing-Cueni[2,6] · Johannes Loffing[2,6] · Bernard Rossier[1,2] · Simona Frateschi[1,2] · Edith Hummler[1,2]

Received: 20 November 2015 / Revised: 21 December 2015 / Accepted: 27 December 2015 / Published online: 14 January 2016

Abstract Aldosterone is the main mineralocorticoid hormone controlling sodium balance, fluid homeostasis, and blood pressure by regulating sodium reabsorption in the aldosterone-sensitive distal nephron (ASDN). Germline loss-of-function mutations of the mineralocorticoid receptor (MR) in humans and in mice lead to the "renal" form of type 1 pseudohypoaldosteronism (PHA-1), a case of aldosterone resistance characterized by salt wasting, dehydration, failure to thrive, hyperkalemia, and metabolic acidosis. To investigate the importance of MR in adult epithelial cells, we generated nephron-specific MR knockout mice ($MR^{Pax8/LC1}$) using a doxycycline-inducible system. Under standard diet, $MR^{Pax8/LC1}$ mice exhibit inability to gain weight and significant weight loss compared to control mice. Interestingly, despite failure to thrive, $MR^{Pax8/LC1}$ mice survive but develop a severe PHA-1 phenotype with higher urinary Na^+ levels, decreased plasma Na^+, hyperkalemia, and higher levels of plasma aldosterone. This phenotype further worsens and becomes lethal under a sodium-deficient diet. Na^+/Cl^- co-transporter (NCC) protein expression and its phosphorylated form are downregulated in the $MR^{Pax8/LC1}$ knockouts, as well as the αENaC protein expression level, whereas the expression of glucocorticoid receptor (GR) is increased. A diet rich in Na^+ and low in K^+ does not restore plasma aldosterone to control levels but is sufficient to restore body weight, plasma, and urinary electrolytes. In conclusion, MR deletion along the nephron fully recapitulates the features of severe human PHA-1. ENaC protein expression is dependent on MR activity. Suppression of NCC under hyperkalemia predominates in a hypovolemic state.

Keywords MR · GR · Thiazide-sensitive Na^+/Cl^- co-transporter · Aldosterone · Salt-losing syndrome

Electronic supplementary material The online version of this article (doi:10.1007/s00424-015-1785-2) contains supplementary material, which is available to authorized users.

✉ Edith Hummler
Edith.Hummler@unil.ch

[1] Department of Pharmacology and Toxicology, University of Lausanne, Rue du Bugnon 27, CH-1011 Lausanne, Switzerland

[2] National Center of Competence in Research "Kidney.CH", Lausanne, Switzerland

[3] Service of Nephrology Department, University Hospital of Lausanne (CHUV), Lausanne, Switzerland

[4] Department of Pharmaceutical Sciences, University of Basel, Basel, Switzerland

[5] Hôpital Tenon, Université Pierre et Marie Curie, Paris, France

[6] Institute of Anatomy, University of Zurich, Zurich, Switzerland

Abbreviations

ASDN	Aldosterone-sensitive distal nephron
MR	Mineralocorticoid receptor
GR	Glucocorticoid receptor
ENaC	Epithelial sodium channel
NCC	Na^+/Cl^- co-transporter
AQP2	Aquaporin 2
Hsd11b2	11β-Hydroxysteroid dehydrogenase type 2
PHA-1	Type 1 pseudohypoaldosteronism
RAAS	Renin-angiotensin-aldosterone system
PCT	Proximal convoluted tubule
PST	Proximal straight tubule
TAL	Thick ascending limb

DCT	Distal convoluted tubule
CNT	Connecting tubule
CCD	Cortical collecting duct

Introduction

MR is expressed not only in Na^+-transporting epithelia such as the kidney and colon [11, 21] but also in non-epithelial tissues (e.g., the heart [20], vessels, and brain [15, 16, 19]). Several inactivating autosomal dominant mutations of the MR gene (*NR3C2*) are the principal cause of renal and sporadic type 1 pseudohypoaldosteronism (PHA-1) which is a rare form of mineralocorticoid resistance characterized by neonatal renal salt wasting, failure to thrive, hyponatremia, hyperkalemia, and metabolic acidosis, accompanied by extremely high values of plasma renin and aldosterone levels. The severe and systemic form of PHA-1 is due to recessive mutations in the genes encoding for the three subunits of the epithelial sodium channel (ENaC) (MIM 600228; MIM 600760; MIM 600761). Germline mineralocorticoid receptor (MR)-deficient mice present a normal prenatal development, but die within 8–12 days after birth from a salt-losing syndrome resembling the human PHA-1. They display hyponatremia, hyperkalemia, hypovolemia, and activation of the renin-angiotensin-aldosterone system (RAAS) with a strong increase in renin, angiotensin II, and aldosterone plasma concentrations. A strong reduction of the activity of ENaC in the colon and kidney was also reported [5]. Interestingly, this phenotype can be rescued by subcutaneous injections of NaCl, although the animals retain their Na^+-losing defect [7]. Inactivation of MR in the principal cells of the late connecting tubule (CNT) and of the collecting duct (CD) driven by the aquaporin 2 (AQP2) promoter can be compensated under a standard sodium diet, but not under a low-sodium diet [23]. This mild phenotype only partially recapitulates the severe human PHA-1 phenotype observed under standard salt diet and was explained by long-term compensatory mechanisms [23]. The same authors used a tamoxifen-inducible strategy to delete MR partially within the CNT and cortical collecting ducts (CCD) during adulthood. Again, only under a low-salt diet and at adult stage, the induced ablation of MR recapitulates the renal sodium wasting observed in mice with constitutive early-onset MR ablation, but not hyperkalemia and/or increased mortality [24]. This was explained by compensatory mechanisms either by upregulation of sodium transporters upstream of the CNT, i.e., the distal convoluted tubule 2 (DCT2) where ENaC and the Na^+/Cl^- co-transporter (NCC) are co-expressed [25] or by upregulation of ENaC-independent, non-electrogenic sodium chloride transporters expressed along the CD [10]. To address this question, we developed an inducible renal tubule-specific MR knockout. Although $MR^{Pax8/LC1}$ mice survive under a standard salt diet, they present with a severe renal PHA-1 phenotype characterized by increased weight loss and urinary Na^+ excretion, hyponatremia, hyperkalemia, high plasma aldosterone levels, and failure to thrive. Our data clearly show that MR expression along the nephron and in the collecting duct system during adulthood is crucial for Na^+ and K^+ homeostasis, and its deletion cannot be compensated neither by sodium transporters including ENaC nor by glucocorticoid receptor (GR) upregulation, but solely by a high Na^+ and low K^+ rescue diet.

Methods

Ethical approval

Animal maintenance and all experimental procedures in mice were in accordance with the Swiss federal guidelines and were approved by the veterinarian local authorities ("Service de la consommation et des affaires vétérinaires") of the Canton de Vaud, Switzerland. Mice were kept in the animal facility under animal care regulations of the University of Lausanne. They were housed in groups of up to five in ventilated cages in a temperature- (23 ± 1 °C) and 60 % humidity-controlled room with an automatic 12-h light/dark cycle. All animals had free access to laboratory chow, and the water was supplied ad libitum. Data origin from both male and female animals. Experiments were performed in 3-week-old animals unless differently stated.

Generation of inducible renal tubule-specific $MR^{Pax8/LC1}$ KO mice

Mice lacking MR all along the nephron and in the collecting duct system of the kidney were generated by using the Pax8-rtTA transgenic mouse line. Triple-transgenic conditional nephron-specific knockouts $Nr3c2^{lox/lox}$; $Pax8\text{-}rtTA^{tg/0}$; $TRE\text{-}LC\text{-}1^{tg/0}$ ($MR^{Pax8/LC1}$) and control littermates $Nr3c2^{lox/lox}$; $Pax8\text{-}rtTA^{tg/0}$ (MR^{Pax8}), $Nr3c2^{lox/lox}$; $TRE\text{-}LC\text{-}1^{tg/0}$ (MR^{LC1}); and $Nr3c2^{lox/lox}$ (MR^{lox}) were obtained by breeding $Nr3c2^{lox/lox}$; $Pax8\text{-}rtTA^{tg/0}$ with $Nr3c2^{lox/lox}$; $TRE\text{-}LC\text{-}1^{tg/0}$ mice. Nr3c2 deletion was induced in renal tubular cells upon doxycycline hydrochloride treatment (Sigma, Deisenhofen, Germany) (2 mg/ml and 2 % sucrose in drinking water) for 15 days in 4-week-old $Nr3c2^{lox/lox}$; $Pax8\text{-}rtTA^{tg/0}$; $TRE\text{-}LC\text{-}1^{tg/0}$ knockout and $Nr3c2^{lox/lox}$; $Pax8\text{-}rtTA^{tg/0}$, $Nr3c2^{lox/lox}$; $TRE\text{-}LC\text{-}1^{tg/0}$ and $Nr3c2^{lox/lox}$ control mice.

Genotyping

DNA was recovered and extracted from mouse biopsies. Genotyping by PCR analysis was performed using the following primers: Pax8-rtTA: ST1 sense (5′-CCATGTCTAGA CTGGACAAGA-3′); ST2 antisense (5′-CTCCAGGCCACA TATGATTAG-3′); LC-1: Cre3 sense (5′-TCGCTGCATT ACCGGTCGATGC-3′); Cre4 antisense (5′-CCATGAGTGA ACGAACCTGGTCG-3′); myogenin: 50S sense (5′-

TTACGTCCATCGTGGACAGC-3′); 51S antisense (5′-TGGGCTGGGTGTTAGTCTTA-3′). Primers for myogenin served as a control for DNA integrity. The PCR program for Pax8-rtTA, TRE-LC-1, and myogenin was the following: 37 cycles, each run consisted of 1 min each at 94, 56, and 72 °C. The knockout band corresponding to the recombination of the floxed Nr3c2 allele and thus MR deletion in the kidney was detected by PCR on the whole kidney using the following primers: MR/Nr3c2: MRflox-1 sense (5′-CTCGAGATC TGAACTCCAGGCT-3′); MRflox-2 antisense (5′-CCTA GAGTTCCTGAGCTGCTGA-3′); MRflox-3 antisense (5′-TAGAAACACTTCGTAAAGTAGAGCT-3′). The PCR program for MR/Nr3c2 was the following: 35 cycles, each run consisted of 30 s at 95 °C followed by 1 min at 63 °C and 1 min at 72 °C.

Quantitative RT-PCR on kidney samples

At the end of the experimentation, mouse kidneys were isolated, frozen in liquid nitrogen, and stored at −80 °C. A tissue-lyser machine (QIAGEN) was used to homogenize the kidney tissues. RNA was extracted from the lysed tissues using the guanidinium thiocyanate-phenol-chloroform extraction method (QIAzol lysis reagent, QIAGEN), and its concentration and quality were measured and evaluated by the Nano Drop (Witec Ag ND-1000 Spectrophotometer). Then, the extracted RNA was used and cDNA was synthetized by retro-transcription using the PrimeScript RT reagent Kit (Takara Bio Inc, Japan). To quantify the relative mRNA expression of MR, 11β-HSD2 and Ren-1^{c}, a real-time PCR (TaqMan) was performed using Applied Biosystems 7500 (Foster City, CA). Primer and probe mix (Mm01241592_mH for MR; Mm01251104_m1 for 11β-HSD2; Mm02342887_mH for Ren-1^{c}; 4352341E for β-Actin) and the TaqMan Gene Expression Master Mix were purchased and used according to the manufacturers' instructions (Applied Biosystem, Foster City, CA). Each measurement was performed in duplicate. For each mRNA transcript detection and the control β-actin, the cDNA, the primers, and the probe were mixed and aliquoted together into the TaqMan Universal PCR Master Mix (Applied Biosystem). Quantification of fluorescence was normalized to β-actin fluorescence to quantify the relative mRNA transcript expression in the whole kidney.

Western blot analysis

Freshly isolated kidneys were homogenized by using a polytron. Homogenates were centrifuged for 10 min at 4 °C at 11,000 rpm. The supernatant was taken, and protein concentration was measured by the Bradford method. Protein extracts from the whole kidney were subjected to Western blot analysis. The proteins were loaded and separated on 10 % polyacrylamide gels by SDS-PAGE, subjected to a constant electric current of 25 mA in running buffer 1×. Then, the proteins were transferred onto a PVDF (Perkin Elmer, Boston, MA) or nitrocellulose membrane (Amersham Hybond-ECL, GE Healthcare) applying a constant current of 100 V during 3 h in transfer buffer 1×. Membranes were subsequently investigated for Nr3c2 (MR), Scnn1a (α-ENaC), Slc12a3 (NCC), phosphorylated Slc12a3 (pT53-NCC), Nr3c1 (GR), and β-actin using primary antibodies Nr3c2 (1:100) [14], Scnn1a (1:500) [26], Slc12a3 (1:500) (Chemicon), pT53-Slc12a3 (1:1000; Pineda Antibody Services), Nr3c1 (1:1000; Santa Cruz, Dallas, TX), β-actin (1:1000; Sigma-Aldrich), anti-rabbit IgG secondary antibody (1:10,000; Amersham, Burkinghampshire, UK), and anti-mouse IgG secondary antibody (1:10,000; Jackson Immuno Research, Baltimore, PA). The secondary antibodies were coupled with horseradish peroxidase (GE Healthcare, Millipore) that allows the revelation of the proteins by chemiluminescence with ECL reagents (GE Healthcare or Pierce, Rockford, IL). Thereby, the membranes were exposed on a photographic film (GE Healthcare, Millipore) during different times in a cassette (Axon Lab) and developed. The films were scanned, and the band intensity was measured using Image Studio Lite software from LI-COR Biosciences.

Immunofluorescence

The kidneys of mice kept under regular salt diet were fixed with 3 % paraformaldehyde and 0.1 % glutaraldehyde in a cacodylate-sucrose buffer as described previously [18]. MR was detected on cryosections by using a primary monoclonal antibody (mouse anti-rat-MR rMR1-18 [14], 1:40) incubated overnight at 4 °C and a secondary antibody goat-anti-mouse HRP (1:50, Jackson ImmunoResearch). The signal was amplified by using the Tyramide Signal Amplification (TSA) System (Perking Elmer). An antigen retrieval treatment was performed by microwave during 10 min in 0.1 M citrate buffer (pH 6). Phosphorylated NCC was detected by using a rabbit-anti-mouse pT53NCC antibody [31] (1:40,000) incubated overnight at 4 °C and a secondary goat-anti-rabbit-CY3 antibody (1:1000, Jackson ImmunoResearch). Staining was performed on 5-μm sections.

Kidney perfusion and microdissection

Mice were anesthetized by a mixture of ketamine/xylazine/acepromazine (100 mg/kg/ 15 mg/kg /2.5 mg/kg) injected intraperitoneally. The perfusion was performed under narcosis into the renal artery by using a catheter. Renal artery perfusion was made by 10 ml of DMEM F-12 (Dulbecco's modified Eagle medium: nutrient mixture F-12) followed by 10 ml liberase (0.9 mg/ml, Liberase Blendzyme 4, Hoffmann-La Roche Inc.). Then, the kidneys were microdissected as described previously [8]. Two centimeters of each segment

(PC, PS, TAL, DCT/CNT, and CD) were recovered and processed for relative protein expression analysis. The microdissection was performed on three experimental and control animals.

Metabolic cage studies

Metabolic balance studies were performed to analyze the renal sodium, potassium, and water homeostasis under normal sodium, sodium-deficient, and high-sodium and low-potassium rescue diets. For time-course analyses, 4- to 6-week-old control and knockout mice from the same litter were individually placed into mouse metabolic cages (Tecniplast, Buguggiate, Italy) and fed with different salt diets for 6 days. During the experimentation, body weight, urine volume, and water and food consumption were determined and urine was collected every day at the same time. Experimental animals had free access to food and water during the experimentations in metabolic cages.

Regular sodium diet

Twenty-three-day-old control and KO mice were individually placed into metabolic cages. Mice were fed with a regular salt diet (0.17 % Na^+ in the food, Ssniff Spezialdiäten GmbH) during the 6 days in the metabolic cages. Doxycycline treatment was started from day 2 (25-day-old) and applied until the end (day 6) of the metabolic cage study.

Sodium-deficient diet

Twenty-five-day-old mice were placed in normal cages and treated with doxycycline for 15 days to induce MR deficiency along the nephron and the collecting duct system. At the end of the doxycycline treatment, control and KO mice were placed into metabolic cages and fed with a regular salt diet (0.17 % Na^+ in the food, Ssniff Spezialdiäten GmbH) for 2 days, followed by 3 days of sodium-deficient diet (0.02 % Na^+ in the food, Ssniff Spezialdiäten GmbH).

High-sodium and low-potassium rescue diet

Twenty-five-day-old mice were placed in normal cages and treated with doxycycline for 15 days to induce MR deficiency along the nephron and the collecting duct system. During these 15 days of doxycycline treatment, mice were fed with a regular sodium diet (0.17 % Na^+ in the food, Ssniff Spezialdiäten GmbH) during the first week and received a high-sodium and low-potassium rescue diet (3.5 % Na^+ in the food, Ssniff Spezialdiäten GmbH, and 0.2 % K^+ in drinking water) throughout the second week. At the end of the doxycycline treatment, control and KO mice were placed into metabolic cages and continued to receive the rescue diet (high Na^+ and low K^+) and had free access to tap water supplemented with 0.2 % of potassium. At the end of the experimentations, blood samples were collected and mice were sacrificed by decapitation. Freshly isolated kidneys were snap-frozen in liquid nitrogen and stored at −80 °C for further molecular analysis.

Urine and plasma analysis

Urine samples (12–24 h) were collected in metabolic cages. At the end of experiments, blood samples were recovered. Urinary and plasma sodium and potassium concentrations were measured using the IL943 Flame Photometer (Instrumentation Laboratory, UK). Plasma aldosterone levels were measured according to standard procedure using the Coat-A-Count RIA kit (Siemens Medical Solutions Diagnostics, Ballerup, Denmark). Moreover, plasma corticosterone levels were quantified as previously described [30]. The urinary and plasmatic creatinine concentration measurements were performed by enzyme-linked immunosorbent assay (ELISA) at the Zurich Integrative Rodent Physiology platform (ZIRP, Zurich, Switzerland) using the UniCel DxC800 system (Beckman Coulter).

Determination of 11β-HSD2 enzyme activity

11β-HSD2 enzyme activity was measured as previously described [4].

Statistical analysis

All measurements were analyzed using the unpaired two-tailed Student's *t* test, considering $MR^{Pax8/LC1}$ KO versus control mice, unless differently stated. Data are presented as mean ± SEM. Values displaying a *P* value smaller than 0.05 were considered as statistically significant, $*P<0.05$; $**P<0.01$; $***P<0.001$; and $^{\#}P<0.0001$.

Results

Generation of inducible nephron-specific $MR^{Pax8/LC1}$ knockout mice

We generated inducible renal tubule-specific MR knockout mice by using the *Nr3c2* floxed allele ($Nr3c2^{lox/lox}$ [6]), the Pax8-rtTA transgenic mice expressing the reverse tetracycline transactivator under the control of the *Pax8* promoter that is driving the expression in all proximal and distal tubular cells along the nephron [32], and the TRE-LC-1 transgenic mice where the expression of the Cre recombinase and luciferase is under the control of the tetracycline response element [28]. The reverse tetracycline transactivator binds and transactivates the tetracycline-responsive element in the presence of doxycycline, thereby triggering Cre recombinase expression and thus deletion of the

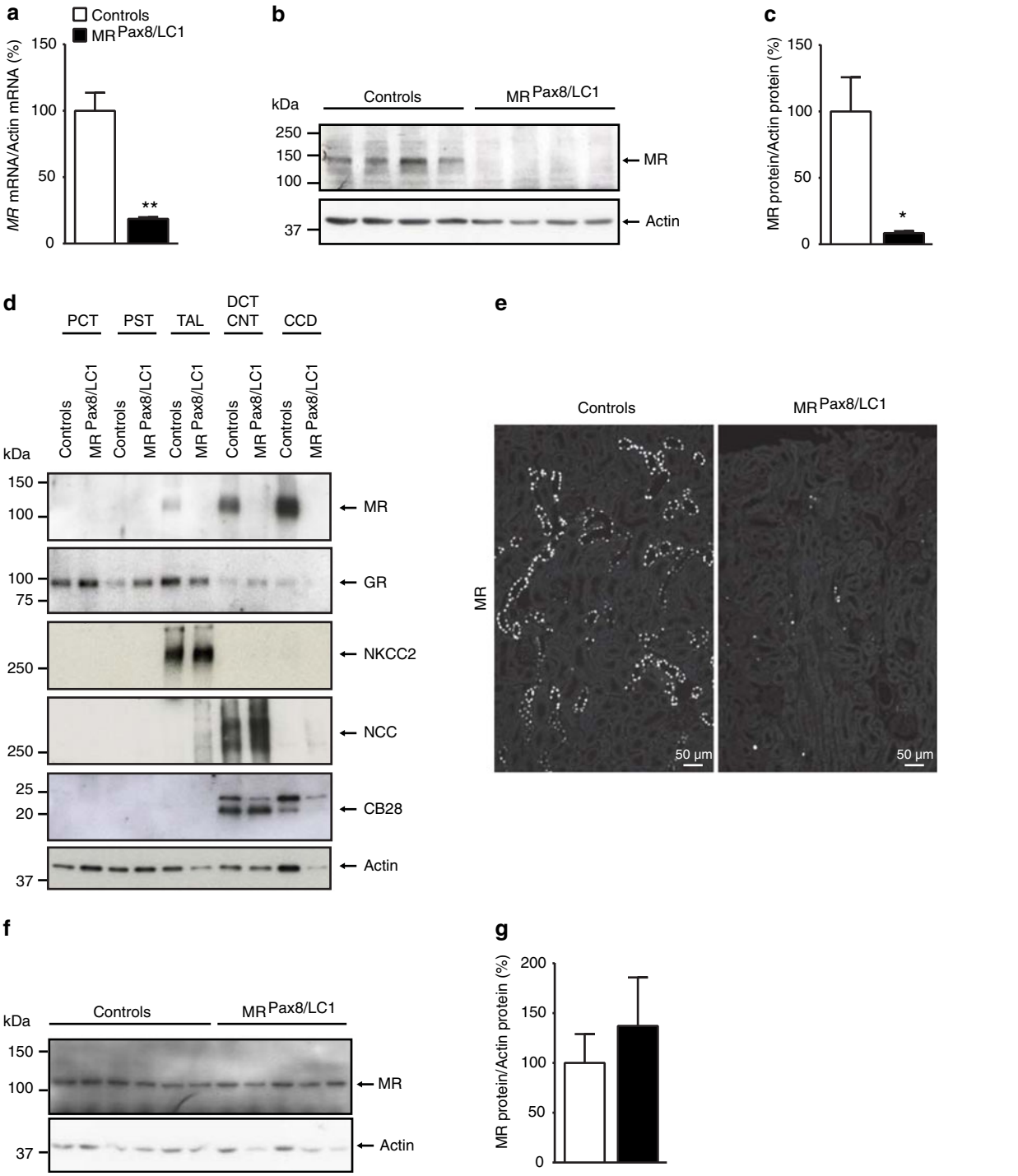

Fig. 1 Characterization of inducible renal tubule-specific $MR^{Pax8/LC1}$ KO mice. **a** Quantification of *Nr3c2* mRNA expression relative to β-actin in the whole kidneys of $MR^{Pax8/LC1}$ KO mice and their control littermates ($n = 4$ per genotype). **b** Analysis of MR protein expression by Western blot analysis in whole kidney lysates. β-Actin was used as loading control ($n = 4$ per genotype). **c** Quantification of MR protein expression relative to β-actin of panel **b. d** Representative analysis of MR protein expression by Western blot analysis from microdissected renal tubules. *PCT* proximal convoluted tubule, *PST* proximal straight tubule, *TAL* thick ascending limb, *DCT* distal convoluted tubule, *CNT* connecting tubule, *CCD* cortical collecting duct. GR expressed throughout the whole nephron, NKCC2 as marker of the TAL, NCC solely expressed in the DCT and CNT, and CB28 as a distal marker of the nephron were used to define the different nephron segments. **e** Representative analysis of MR protein expression by immunofluorescence from total kidney under regular sodium diet ($n = 4$ per genotype). **f** Analysis of MR protein expression by Western blot analysis in whole liver lysates in KO ($n = 5$) and control ($n = 6$) mice. **g** Quantification of MR protein expression in the liver relative to β-actin of panel **e**

floxed allele. We treated 4-week-old $MR^{Pax8/LC1}$ triple transgenic animals (carrying the $Nr3c2^{lox/lox}$, Pax8-$rtTA^{tg/0}$, and TRE-LC-$1^{tg/0}$ transgenes and named $MR^{Pax8/LC1}$) and their control littermates ($Nr3c2^{lox/lox}$; Pax8-$rtTA^{tg/0}$, $Nr3c2^{lox/lox}$; TRE-LC-$1^{tg/0}$, and $Nr3c2^{lox/lox}$ named MR^{Pax8}, MR^{LC1}, and MR^{lox}, respectively) with doxycycline to induce the deletion of the *Nr3c2* gene locus in adult mice. Quantitative mRNA expression measurement of MR revealed an 80 % decrease in $MR^{Pax8/LC1}$ knockout mice (Fig. 1a), and Western blot analyses showed a 90 % reduction of Nr3c2 protein expression upon doxycycline treatment in the whole kidney (Fig. 1b, c). Western blot analyses of microdissected nephron segments confirmed wild-type MR expression in the distal nephron, namely the thick ascending limb (TAL), distal convoluted tubule (DCT), connecting tubule (CNT), and in the cortical collecting ducts (CCD) in control mice and demonstrated absence of MR protein expression in the corresponding segments of the $MR^{Pax8/LC1}$ knockout mice (Fig. 1d and Supplementary Fig. 1). The glucocorticoid receptor GR, the cotransporter NKCC2, the sodium-chloride symporter NCC, and the cytoplasmic Ca^{2+}-binding protein calbindin CB28 were used as markers of the different nephron segments (Fig. 1d). A strong reduction in MR expression in the $MR^{Pax8/LC1}$ knockout mice could also be demonstrated by immunofluorescence (Fig. 1e). Pax8 expression has been described also in the liver

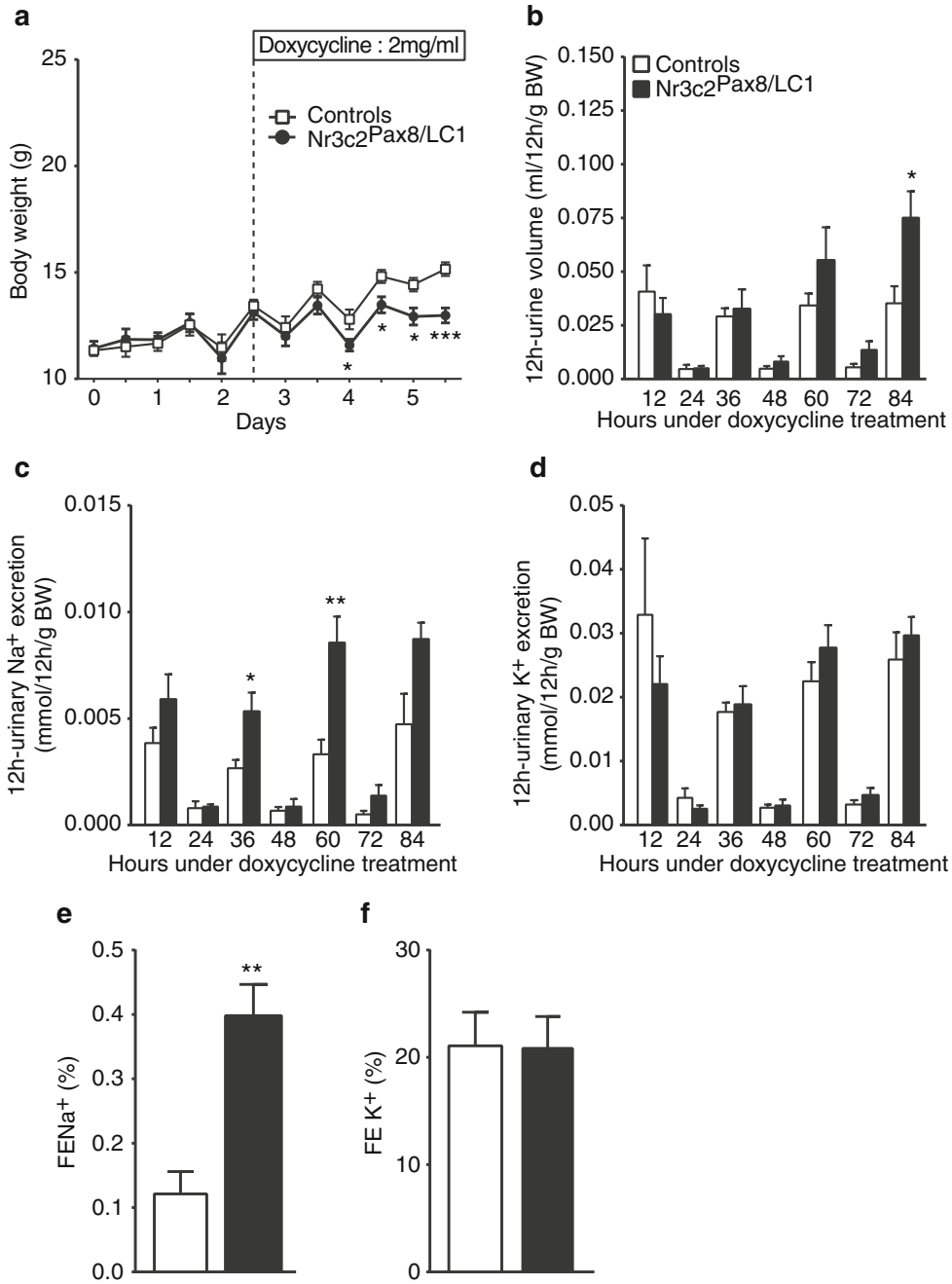

Fig. 2 Weight loss, increased urine volume and urinary sodium excretion under regular sodium diet. **a** Body weight of $MR^{Pax8/LC1}$ KO and control mice before and following doxycycline treatment ($n = 7$ per genotype). **b**, **c**, **d** Time course for 12-h urine volume (**b**), urinary sodium excretion (**c**), urinary potassium excretion (**d**). **e**, **f** Fractional excretion (*FE*) of Na^+ ($n = 5$–6 per genotype) (**e**) and fractional excretion of K^+ ($n = 7$ per genotype) (**f**) determined 2 weeks after doxycycline treatment in metabolic cages for $MR^{Pax8/LC1}$ KO and control mice under regular sodium diet

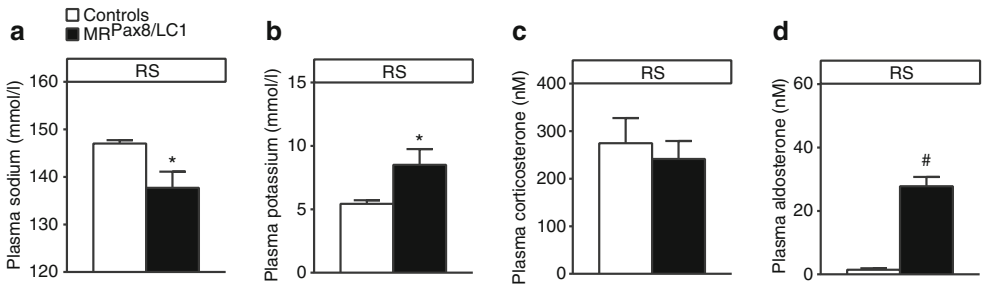

Fig. 3 Decreased plasma sodium levels, hyperkalemia, and increased plasma aldosterone levels under normal salt diet. **a**, **b** Plasma sodium (**a**) and potassium (**b**) concentrations in $MR^{Pax8/LC1}$ KO ($n=7$) and control ($n=9$) mice following 4 days of doxycycline treatment. **c**, **d** Plasma corticosterone (**c**) and aldosterone (**d**) levels measured in KO ($n=8$–11) and control ($n=8$–11) animals following 15 and 4 days of doxycycline treatment, respectively. *RS* regular sodium diet, 0.17 % Na^+ in food

[32], but we observed no changes of MR protein expression in this organ (Fig. 1f, g).

Adult nephron-specific $MR^{Pax8/LC1}$ knockout mice develop a PHA-1 phenotype under a regular sodium diet

We monitored the body weight of $MR^{Pax8/LC1}$ knockout and control animals fed with a regular salt diet. $MR^{Pax8/LC1}$ knockout mice rapidly stopped to gain body weight, whereas control animals kept gaining weight (Fig. 2a) following the doxycycline induction. To determine urinary and plasma Na^+ and K^+ concentrations, we placed control and knockout animals into metabolic cages and performed measurements every 12 h to evaluate the cyclicity of sodium, potassium, and water excretion. $MR^{Pax8/LC1}$ knockout mice exhibited increased urine volume output and urinary Na^+ excretion under a standard salt diet (Fig. 2b, c), while the urinary K^+ excretion did not change (Fig. 2d). Interestingly, these differences are obvious only during the activity period (night) (Fig. 2b, c). The fractional excretion of K^+ did not vary between the two groups as well as the absolute K^+ excretion (controls 0.023 ± 0.003 mmol/24 h/g, $n=6$ and knockouts 0.022 ± 0.0021 mmol/24 h/g, $n=6$), while the

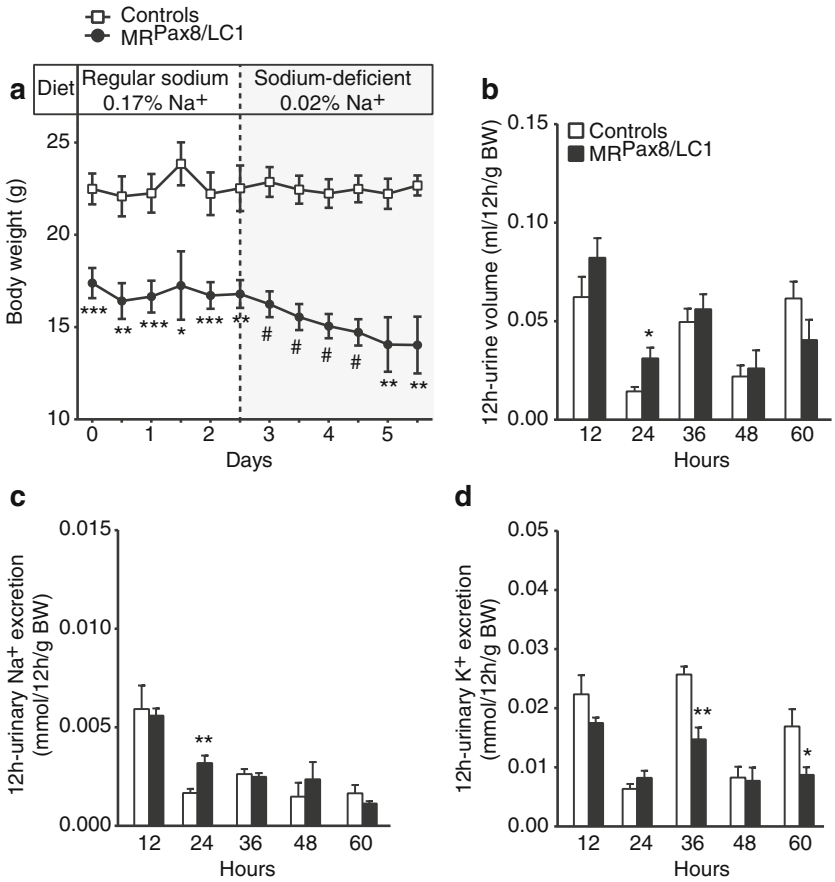

Fig. 4 Continuous body weight loss and decreased urinary potassium excretion upon sodium-deficient diet. **a** Body weight under standard salt diet followed by a sodium-deficient diet. KO ($n=9$) and controls ($n=8$). **b**, **c**, **d** Time course for 12-h urine volume (**b**), urinary sodium excretion (**c**), and urinary potassium excretion (**d**) determined in metabolic cages in KO ($n=9$) and control ($n=8$) animals receiving a sodium-deficient diet

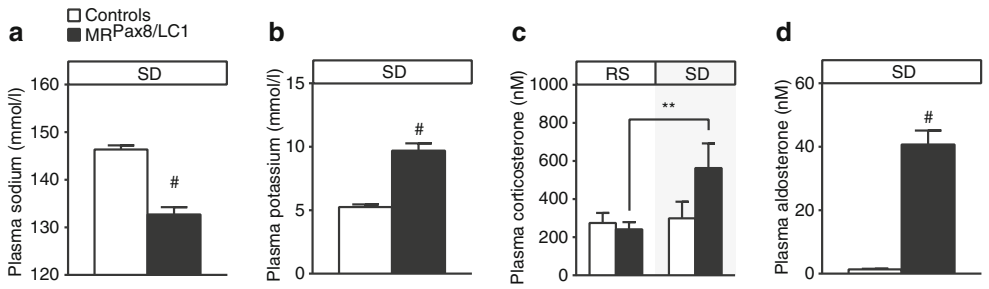

Fig. 5 Hyponatremia, hyperkalemia, and highly increased plasma aldosterone levels under sodium-deficient diet. **a**, **b** Plasma sodium (**a**) and potassium (**b**) concentrations following 15 days of doxycycline treatment, KO ($n = 12$) and controls ($n = 15$). **c**, **d** Plasma corticosterone (**c**) and plasma aldosterone (**d**) levels following 15 days of doxycycline treatment ($n = 8$–9 per genotype). *RS* regular sodium diet, 0.17 % Na^+ in food, *SD* sodium-deficient diet, 0.02 % Na^+ in food. $^{**}P < 0.01$, KO under Na^+-deficient versus KO under regular Na^+ diet

fractional excretion of Na^+ was significantly increased in the knockouts (Fig. 2e, f), confirming that the increase in urinary sodium excretion reported in Fig. 2c is not transient but sustained upon regular sodium diet several weeks after MR deletion in renal tubules. $MR^{Pax8/LC1}$ knockout animals also presented with significantly lower natremia but still within the physiological range (135–145 mmol/l) and hyperkalemia (Fig. 3a, b). We observed no difference in food intake (Supplementary Table 1) and in plasma corticosterone levels (Fig. 3c). Urine creatinine concentration did not vary among the two groups (Supplementary Fig. 2A); however, plasma creatinine concentration was significantly higher (Supplementary Fig. 2B) and the creatinine clearance significantly reduced (Supplementary Fig. 2C) in the knockout animals indicating that kidney function is affected by the loss of MR in renal tubules. Moreover, plasma aldosterone levels markedly increased in the $MR^{Pax8/LC1}$ knockouts (Fig. 3d), mimicking a severe PHA-1 phenotype.

The PHA-1 phenotype becomes lethal under a sodium-deficient diet

The shift to a diet deficient in Na^+ caused a further severe decrease in the body weight of the knockout animals (Fig. 4a) after 3 days of diet shift ($n = 9$, $MR^{Pax8/LC1}$ knockouts). Water

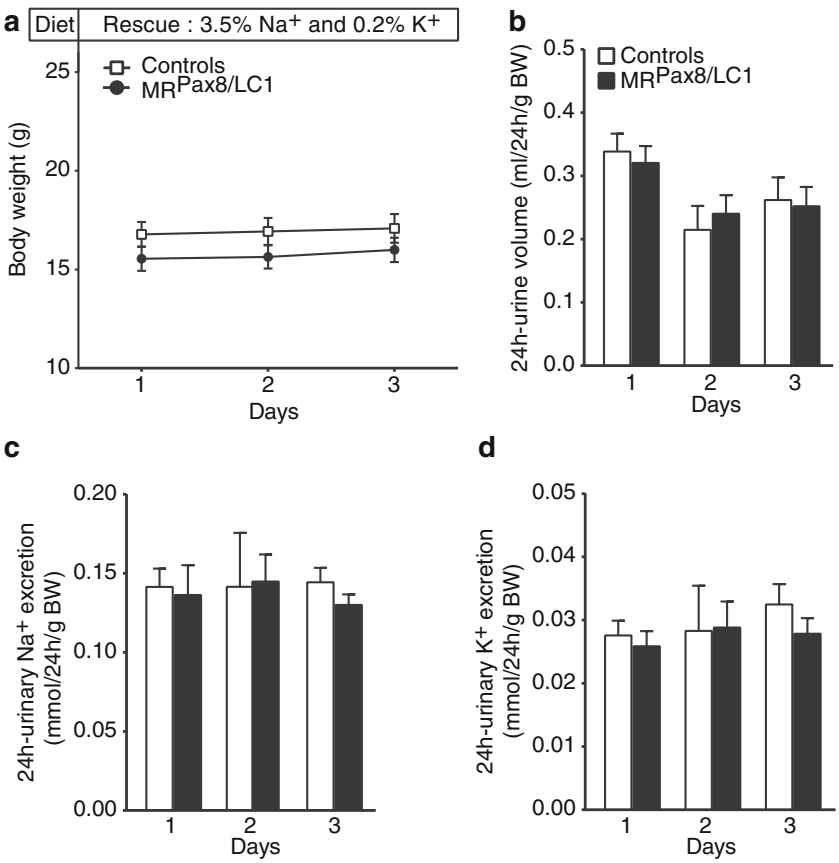

Fig. 6 Restoration of body weight and urinary electrolytes upon a high-sodium and low-potassium (rescue) diet. **a** Body weight of $MR^{Pax8/LC1}$ KO and control mice upon a high-sodium and low-potassium diet ($n = 11$ per genotype). **b**, **c**, **d** Time course for 24-h urine volume (**b**), urinary sodium excretion (**c**), and urinary potassium excretion (**d**) determined in metabolic cages for $MR^{Pax8/LC1}$ KO and control mice under a high-sodium and low-potassium diet ($n = 5$ per genotype)

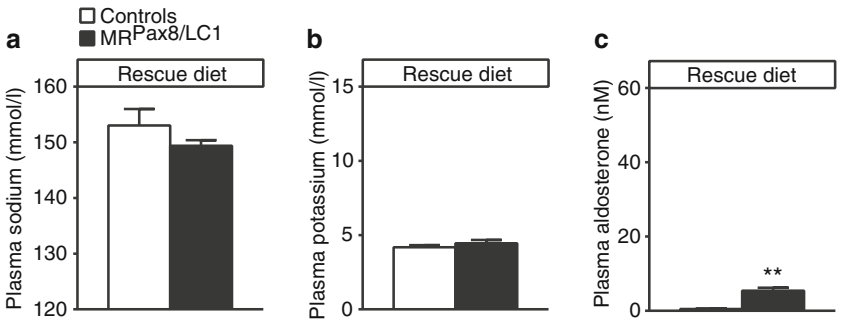

Fig. 7 Restoration of plasma electrolytes upon high-sodium and low-potassium (rescue) diet. **a**, **b** Plasma sodium (**a**) and potassium (**b**) concentrations in $MR^{Pax8/LC1}$ KO ($n = 6$) and control ($n = 5$) mice under a high-sodium and low-potassium diet. **c** Plasma aldosterone levels measured in KO ($n = 6$) and control ($n = 5$) animals under a high-sodium and low-potassium diet. Measurements were performed following 15 days of doxycycline treatment and 15 days of rescue diet

and food consumption did not change (Supplementary Table 1); however, urine volume and urinary Na^+ excretion were increased and urinary K^+ excretion was significantly reduced in the $MR^{Pax8/LC1}$ knockout animals (Fig. 4b–d) which also presented with hyponatremia and hyperkalemia (Fig. 5a, b). Plasma corticosterone levels in the knockout animals increased following the shift from a regular Na^+ diet to a Na^+-deficient diet (Fig. 5c). Plasma aldosterone further increased in the $MR^{Pax8/LC1}$ knockout mice under a sodium-deficient diet (Fig. 5d) to reach extraordinarily high levels (40 nM), a concentration that should occupy 100 % of MR and a significant proportion (about 20 %) of GR [12].

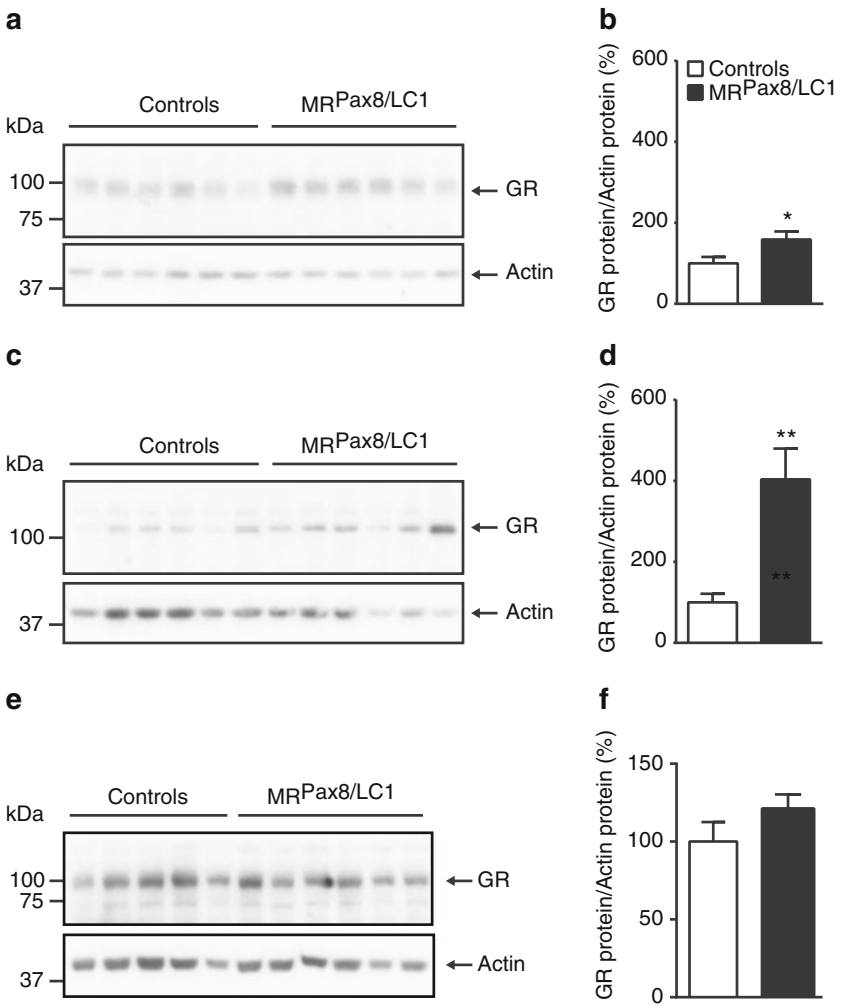

Fig. 8 Increased GR protein levels upon regular and sodium-deficient diets. **a** Representative Western blot analysis of GR and β-actin in whole kidney lysates under a regular sodium diet ($n = 6$ per genotype). **b** Graph shows quantification of Western blots for GR from two independent experiments. **c** Representative Western blot analysis of GR and β-actin in whole kidney lysates under a sodium-deficient diet ($n = 6$ per genotype). **d** Graph shows quantification of Western blots in **c.** **e** Representative Western blot analysis of GR and β-actin in whole kidney lysates under a rescue (high Na^+/low K^+) diet ($n \geq 5$ per genotype). **f** Graph shows quantification of Western blots in **e**

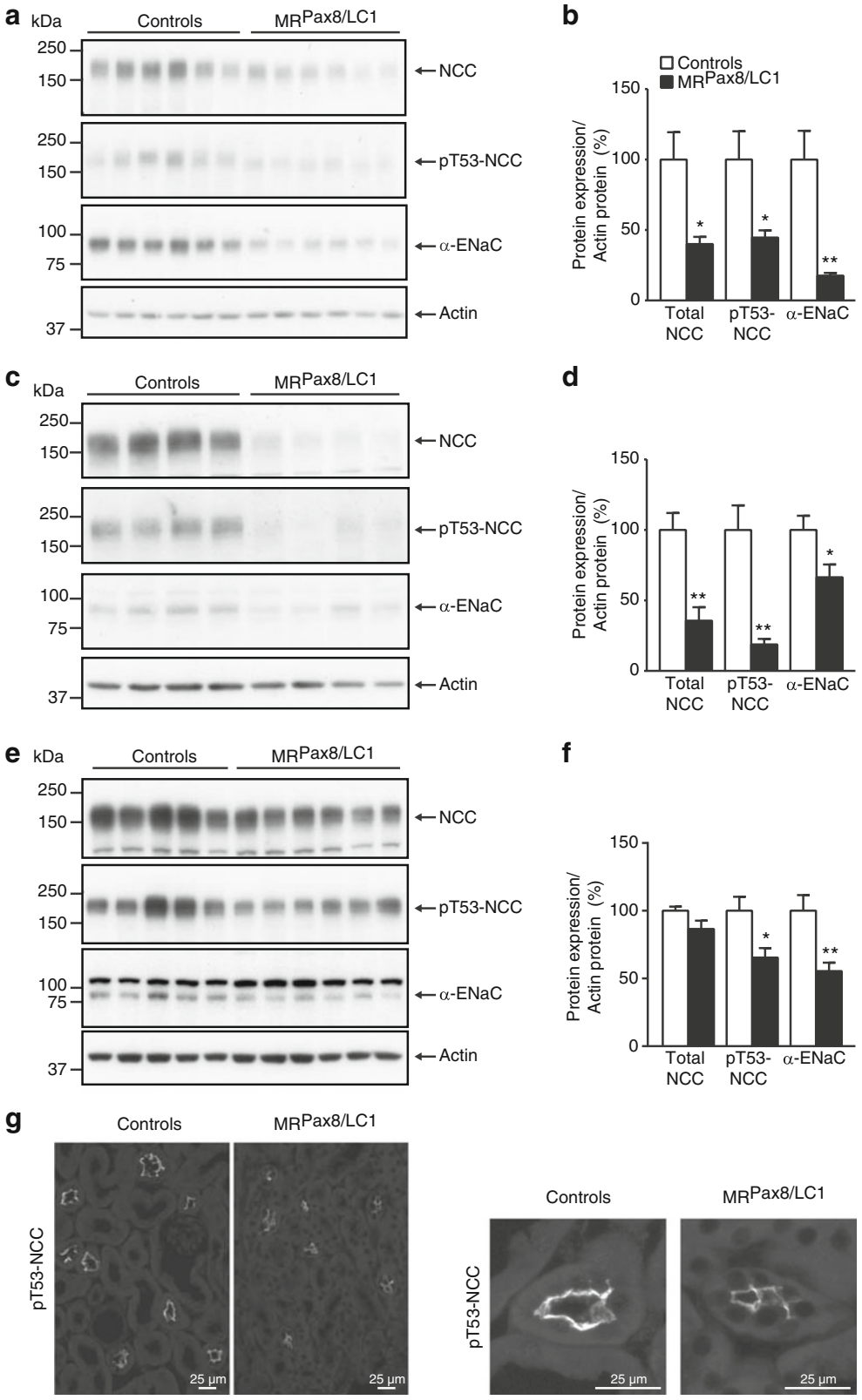
a
kDa
Controls
MRPax8/LC1
250
150
NCC
pT53-NCC
100
75
α-ENaC
37
Actin
b
Controls
MRPax8/LC1
Protein expression/ Actin protein (%)
Total NCC
pT53-NCC
α-ENaC
c
d
e
f
g
pT53-NCC
25 μm

◀ **Fig. 9** Downregulation of NCC and α-ENaC protein expression. **a** Representative Western blot analysis for total NCC, phosphorylated pT53-NCC, and α-ENaC in kidney lysates from mice kept under regular sodium diet. β-Actin was used as loading control ($n = 6$ per genotype). **b** Graphs show quantification of Western blots for NCC, pT53-NCC, and α-ENaC from two independent experiments and normalized to *β-actin* ($n = 7$ per genotype). KO and control animals were kept upon regular sodium diet, and proteins were extracted from the whole kidney. **c** Western blot analyses for total NCC, phosphorylated pT53-NCC, and α-ENaC in kidney lysates from mice kept under sodium-deficient diet during 3 days. β-Actin was used as loading control ($n = 4$ per genotype). **d** Graphs show quantification of Western blots for NCC, pT53-NCC, and α-ENaC from two independent experiments and normalized to *β-actin* ($n = 7$ per genotype). KO and control animals were kept upon sodium-deficient diet, and proteins were extracted from the whole kidney. **e** Western blot analysis for total NCC, phosphorylated pT53-NCC, and α-ENaC in kidney lysates from mice kept under high-Na^+/low-K^+ rescue diet. β-Actin was used as loading control ($n \geq 5$ per genotype). **f** Graphs show quantification of Western blots in **e. g** Analysis of phospho-NCC protein expression by immunofluorescence from total kidney ($n = 4$ per genotype) upon regular sodium diet

High-Na^+ and low-K^+ diet restores body weight and electrolyte balance in $MR^{Pax8/LC1}$ knockout mice

To counterbalance for Na^+ loss and reduced K^+ excretion, nephron-specific $MR^{Pax8/LC1}$ knockout mice were subjected to a diet rich in Na^+ and low in K^+ during 2 weeks. Indeed, the knockout animals restored body weight gain compared to controls following high-Na^+ and low-K^+ treatment (Fig. 6a). Food and water intake (Supplementary Table 1), urinary and plasma Na^+ and K^+ concentrations, and urine volume were indistinguishable between the two groups (Fig. 6b–d and Fig. 7a, b), but plasma aldosterone levels of $MR^{Pax8/LC1}$ knockout animals remained significantly higher following high-Na^+ and low-K^+ diet (Fig. 7c). Thus, solely a diet rich in Na^+ and low in K^+ allows the $MR^{Pax8/LC1}$ knockout mice to develop normally and to restore urine and plasma electrolytes.

Increased GR expression in the $MR^{Pax8/LC1}$ knockout mice

Being both expressed in the ASDN, GR and MR have been proposed to have opposing effects, suggesting that activated GR can partially but not completely compensate for the loss of MR function [5, 23, 27, 29]. We thus analyzed GR protein expression in the kidneys of $MR^{Pax8/LC1}$ knockout mice by Western blot analyses. We found a moderate but significant increase in the protein expression of GR under normal Na^+ diet (Fig. 8a, b). This increase was less obvious at the cellular level, as revealed by immunofluorescence analyses, and may be restricted to specific cell types (data not shown). Under Na^+-deficient diet, GR protein expression was about four times significantly increased in the knockouts (Fig. 8c, d) indicating that MR deletion leads to increased renal expression of GR. This increase is absent following the rescue (high Na^+/low K^+) diet (Fig. 8e, f). Furthermore, mRNA levels of the 11β-hydroxysteroid dehydrogenase (Hsd11b2) and renin ($Ren\text{-}1^c$) were significantly increased in the kidney of $MR^{Pax8/LC1}$ knockout mice under both normal and Na^+-deficient diets (Supplementary Fig. 3A-D); however, the activity of the enzyme 11β-hydroxysteroid dehydrogenase type 2 (Hsd11b2) did not vary (Supplementary Fig. 3E).

Decreased NCC activity in the $MR^{Pax8/LC1}$ knockout mice despite severe salt-losing syndrome

To study whether the absence of MR in adult kidneys might regulate the expression and function of sodium-transporting proteins, we analyzed NCC and ENaC protein expression following induction of MR deficiency under standard, Na^+-deficient and rescue (high Na^+/low K^+) diets. $MR^{Pax8/LC1}$ knockout mice presented with a significant decrease in the levels of total and phosphorylated NCC, and this decrease was even more pronounced under a Na^+-deficient diet (Fig. 9a–d), but less important under the rescue diet (Fig. 9e, f). Immunofluorescence staining of perfused kidneys also revealed a decreased phospho-NCC expression in $MR^{Pax8/LC1}$ knockout mice under a standard salt diet (Fig. 9g). The protein expression of the α subunit of ENaC was also significantly reduced in the knockout animals (Fig. 9a–f). Altogether, these data indicate that the absence of MR in the nephron leads to NCC downregulation despite the increased sodium loss.

Discussion

We focused our study on the acute deletion of MR along the entire nephron and the collecting ducts of adult animals by using the Pax8-rtTA; TRE-LC-1 double transgenic mice [32]. $MR^{Pax8/LC1}$ knockout mice present failure to thrive as a result of increased renal loss of sodium and water. The mutant mice also show highly increased plasma aldosterone levels on both standard and Na^+-deficient diets, developing a severe pseudohypoaldosteronism syndrome with rapid weight loss, disturbance of plasma Na^+ and K^+ concentrations, and significantly increased urinary Na^+ loss and decreased K^+ excretion (Figs. 2, 3, 4, and 5). The phenotype observed in the $MR^{Pax8/LC1}$ knockout mice is more severe than that observed in mice deficient for MR in renal principal cells in which inactivation of MR in CD and late CNT does not affect Na^+ balance under standard conditions [23, 24]. The results presented in this article clearly demonstrate that MR deficiency in the nephron during adulthood cannot be compensated by sodium transporting proteins upstream of late CNT (NCC [13]) or downstream along the CD (electroneutral sodium chloride reabsorption [10]), and that MR expression either in the TAL, DCT, or intercalated cells is crucial to maintain Na^+ and K^+ homeostasis.

Both MR and GR are expressed in the distal renal tubular cells [1] and can bind and be activated by the mineralocorticoid aldosterone and the glucocorticoid cortisol (corticosterone in

mice and rats), respectively [12, 17]. However, GR can also be bound and activated by aldosterone [12], which is a relatively weak GR agonist with a K_i of 140 nM [22]. Aldosterone stimulates also the transcriptional activity of GR at high concentrations [22]. Yet, in the $MR^{Pax8/LC1}$ knockouts, plasma aldosterone rises to a maximum of 40 nM (Figs. 3d and 5d). MR can also be bound and activated by cortisol (corticosterone in mice and rats), but since physiological glucocorticoids circulate in the blood at 100–1000 higher concentration than aldosterone, rapid conversion of cortisol to cortisone by the enzyme 11β-hydroxysteroid dehydrogenase type 2 (11βHSD2) allows aldosterone to selectively activate MR in epithelial tissues. In vitro and in vivo experimental models show that GR might play a role in renal sodium transport [3] being implicated in compensatory [5] or cooperative [12] mechanisms along with MR, and we thus hypothesized that GR in $MR^{Pax8/LC1}$ knockout mice might compensate at least partially for the loss of MR. We found however no compensatory action of GR on MR in the context of renal salt transport, that could not be confirmed by immunochemistry under a regular salt diet (data not shown). This occurred despite an overall increased GR protein expression in the kidney of the $MR^{Pax8/LC1}$ knockout mice (Fig. 8a, b) and the increased plasma corticosterone levels of the knockouts following the shift to a Na^+-deficient diet (Fig. 5c).

Sodium reabsorption in the aldosterone-responsive distal tubular segments is mediated by the amiloride-sensitive epithelial sodium channel ENaC expressed in the principal cells of the CD and CNT, together with the thiazide-sensitive sodium-chloride co-transporter NCC in the DCT [25]. Described as the "aldosterone paradox," aldosterone can either trigger Na^+ reabsorption in the DCT via the Na^+/Cl^- co-transporter NCC and ENaC in DCT2, CNT, and CD following a hypovolemic challenge or increase NaCl delivery by inhibiting NCC activity in DCT responding to an hyperkalemic challenge. This results in differential regulation of Na^+ and K^+ transport between the DCT and the ASDN [2]. Aldosterone can activate ENaC through MR by inhibiting Nedd4-2 via phosphorylation by serum- and glucocorticoid-induced kinase 1 (Sgk1) [9], but aldosterone-activated MR can also bind to the promoter region of the gene encoding the α subunit of ENaC leading to de novo synthesis of this channel [33]. We found a reduction in the expression of the αENaC protein in $MR^{Pax8/LC1}$-deficient mice under normal, low-Na^+, and high-Na^+/low-K^+ rescue diets, showing that ENaC expression is under direct control of MR (Fig. 9). As the knockout animals suffer from Na^+ wasting, they could be in a hypovolemic state, and thus, both hypovolemia and hyperkalemia may be present in the mutant animals. Aldosterone, which is highly increased in the knockouts, should activate NCC, but NCC is significantly less expressed and phosphorylated in the $MR^{Pax8/LC1}$ mice (Fig. 9). This finding is surprising, as the $MR^{Pax8/LC1}$ mice suffer from hyponatremia accompanied by high plasma aldosterone levels, and is consistent with the notion that the hyperkalemic challenge dominates the hypovolemic stimulus in the context of the aldosterone paradox. We also found, surprisingly, no decreased K^+ excretion under a standard diet (Fig. 2f) linked with hyperkalemia. This result was confirmed in three independent series of experiments (data not shown) and by measurements of urinary K^+ fractional excretion (Fig. 2f). One possible explanation could be a reduced but still sufficient ENaC activity to allow normal urinary K^+ excretion. However, this unchanged urinary K^+ excretion in the $MR^{Pax8/LC1}$ knockout mice is not sufficient to avoid the establishment of the hyperkalemic status.

Targeted inactivation of MR in the whole nephron and the collecting duct system with the exception of the glomeruli cannot be compensated on a standard diet by activation of the RAAS, which is reflected by upregulation of $Ren\text{-}1^c$ expression in the kidney and the increased aldosterone levels in the blood of the $MR^{Pax8/LC1}$ knockout mice (Suppl. Fig. 2 and Figs. 2 and 5). The decrease of NCC expression and phosphorylation (Fig. 9) might be induced in an attempt to increase the Na^+ delivery to the CNT and CD where ENaC is normally highly expressed, allowing the exchange of Na^+ against K^+. Thus, apical electrogenic ENaC-mediated transepithelial Na^+ reabsorption allows the excretion of K^+ from principal cells to the primary urine. However, inward Na^+ and outward K^+ transcellular fluxes are impaired in the $MR^{Pax8/LC1}$ knockout mice. Indeed, increased plasma aldosterone levels cannot activate MR in the $MR^{Pax8/LC1}$ knockouts, and thus, aldosterone cannot trigger de novo synthesis of ENaC and ensure the channel stability at the apical membrane via the Sgk1 pathway.

In conclusion, the $MR^{Pax8/LC1}$ knockout mice fully reproduce the human PHA-1 phenotype, ENaC expression is dependent on MR activity, and hyperkalemia is probably the main complication to be avoided even at the expense of increased Na^+ excretion.

Acknowledgments The authors would like to thank Günter Schütz and Stefan Berger for kindly providing us with the $Nr3c2^{lox/lox}$ mouse line and Celso E. Gomez-Sanchez for the antibody against MR. We also like to thank Denise Kratschmar for LC-MS steroid measurements and Anne-Marie Mérillat for figure editing. Moreover, the authors would like to thank all of the members of the laboratory of Edith Hummler for helpful and interactive discussions. Finally, the authors would like to acknowledge the contribution of the COST Action ADMIRE BM1301.

Compliance with ethical standards Animal maintenance and all experimental procedures in mice were in accordance with the Swiss federal guidelines and were approved by the veterinarian local authorities ("Service de la consommation et des affaires vétérinaires") of the Canton de Vaud, Switzerland.

Conflict of interest The authors declare that they have no competing interests.

Funding This work was supported by the Swiss National Center of Competence in Research (NCCR Kidney CH) and the Swiss National Science Foundation (grants SNF 31003A_144198/1 and 31003A_163347/1 to Edith Hummler, 31003A_159454 to Alex Odermatt and 310030_143929 to Johannes Loffing).

References

1. Ackermann D, Gresko N, Carrel M, Loffing-Cueni D, Habermehl D, Gomez-Sanchez C, Rossier BC, Loffing J (2010) In vivo nuclear translocation of mineralocorticoid and glucocorticoid receptors in rat kidney: differential effect of corticosteroids along the distal tubule. Am J Physiol Renal Physiol 299:F1473–F1485. doi:10.1152/ajprenal.00437.2010
2. Arroyo JP, Ronzaud C, Lagnaz D, Staub O, Gamba G (2011) Aldosterone paradox: differential regulation of ion transport in distal nephron. Physiology 26:115–123. doi:10.1152/physiol.00049.2010
3. Bailey MA, Griffin KJ, Scott DJ (2014) Clinical assessment of patients with peripheral arterial disease. Semin Interv Radiol 31:292–299. doi:10.1055/s-0034-1393964
4. Balazs Z, Schweizer RA, Frey FJ, Rohner-Jeanrenaud F, Odermatt A (2008) DHEA induces 11β-HSD2 by acting on CCAAT/enhancer-binding proteins. J Am Soc Nephrol 19:92–101. doi:10.1681/ASN.2007030263
5. Berger S, Bleich M, Schmid W, Cole TJ, Peters J, Watanabe H, Kriz W, Warth R, Greger R, Schutz G (1998) Mineralocorticoid receptor knockout mice: pathophysiology of Na^+ metabolism. Proc Natl Acad Sci U S A 95:9424–9429
6. Berger S, Wolfer DP, Selbach O, Alter H, Erdmann G, Reichardt HM, Chepkova AN, Welzl H, Haas HL, Lipp HP, Schutz G (2006) Loss of the limbic mineralocorticoid receptor impairs behavioral plasticity. Proc Natl Acad Sci U S A 103:195–200. doi:10.1073/pnas.0503878102
7. Bleich M, Warth R, Schmidt-Hieber M, Schulz-Baldes A, Hasselblatt P, Fisch D, Berger S, Kunzelmann K, Kriz W, Schutz G, Greger R (1999) Rescue of the mineralocorticoid receptor knock-out mouse. Pflugers Arch - Eur J Physiol 438:245–254
8. Christensen BM, Perrier R, Wang Q, Zuber AM, Maillard M, Mordasini D, Malsure S, Ronzaud C, Stehle JC, Rossier BC, Hummler E (2010) Sodium and potassium balance depends on alphaENaC expression in connecting tubule. J Am Soc Nephrol 21:1942–1951. doi:10.1681/ASN.2009101077
9. Debonneville C, Flores SY, Kamynina E, Plant PJ, Tauxe C, Thomas MA, Munster C, Chraibi A, Pratt JH, Horisberger JD, Pearce D, Loffing J, Staub O (2001) Phosphorylation of Nedd4-2 by Sgk1 regulates epithelial Na^+ channel cell surface expression. EMBO J 20:7052–7059. doi:10.1093/emboj/20.24.7052
10. Eladari D, Chambrey R, Picard N, Hadchouel J (2014) Electroneutral absorption of NaCl by the aldosterone-sensitive distal nephron: implication for normal electrolytes homeostasis and blood pressure regulation. Cell Mol Life Sci 71:2879–2895. doi:10.1007/s00018-014-1585-4
11. Funder JW, Feldman D, Edelman IS (1973) The roles of plasma binding and receptor specificity in the mineralocorticoid action of aldosterone. Endocrinology 92:994–1004. doi:10.1210/endo-92-4-994
12. Gaeggeler HP, Gonzalez-Rodriguez E, Jaeger NF, Loffing-Cueni D, Norregaard R, Loffing J, Horisberger JD, Rossier BC (2005) Mineralocorticoid versus glucocorticoid receptor occupancy mediating aldosterone-stimulated sodium transport in a novel renal cell line. J Am Soc Nephrol 16:878–891. doi:10.1681/ASN.2004121110
13. Gamba G (2012) Regulation of the renal Na^+- Cl^- cotransporter by phosphorylation and ubiquitylation. Am J Physiol Renal Physiol 303:F1573–F1583. doi:10.1152/ajprenal.00508.2012
14. Gomez-Sanchez CE, de Rodriguez AF, Romero DG, Estess J, Warden MP, Gomez-Sanchez MT, Gomez-Sanchez EP (2006) Development of a panel of monoclonal antibodies against the mineralocorticoid receptor. Endocrinology 147:1343–1348. doi:10.1210/en.2005-0860
15. Gomez-Sanchez EP, Gomez-Sanchez CE (2012) Central regulation of blood pressure by the mineralocorticoid receptor. Mol Cell Endocrinol 350:289–298. doi:10.1016/j.mce.2011.05.005
16. Koenig JB, Jaffe IZ (2014) Direct role for smooth muscle cell mineralocorticoid receptors in vascular remodeling: novel mechanisms and clinical implications. Curr Hypertens Rep 16:427. doi:10.1007/s11906-014-0427-y
17. Krozowski ZS, Funder JW (1983) Renal mineralocorticoid receptors and hippocampal corticosterone-binding species have identical intrinsic steroid specificity. Proc Natl Acad Sci U S A 80:6056–6060
18. Loffing J, Loffing-Cueni D, Valderrabano V, Klausli L, Hebert SC, Rossier BC, Hoenderop JG, Bindels RJ, Kaissling B (2001) Distribution of transcellular calcium and sodium transport pathways along mouse distal nephron. Am J Physiol Renal Physiol 281:F1021–F1027
19. McGraw AP, McCurley A, Preston IR, Jaffe IZ (2013) Mineralocorticoid receptors in vascular disease: connecting molecular pathways to clinical implications. Curr Atheroscler Rep 15:340. doi:10.1007/s11883-013-0340-x
20. Messaoudi S, Azibani F, Delcayre C, Jaisser F (2012) Aldosterone, mineralocorticoid receptor, and heart failure. Mol Cell Endocrinol 350:266–272. doi:10.1016/j.mce.2011.06.038
21. Pressley L, Funder JW (1975) Glucocorticoid and mineralocorticoid receptors in gut mucosa. Endocrinology 97:588–596. doi:10.1210/endo-97-3-588
22. Rebuffat AG, Tam S, Nawrocki AR, Baker ME, Frey BM, Frey FJ, Odermatt A (2004) The 11-ketosteroid 11-ketodexamethasone is a glucocorticoid receptor agonist. Mol Cell Endocrinol 214:27–37. doi:10.1016/j.mce.2003.11.027
23. Ronzaud C, Loffing J, Bleich M, Gretz N, Grone HJ, Schutz G, Berger S (2007) Impairment of sodium balance in mice deficient in renal principal cell mineralocorticoid receptor. J Am Soc Nephrol 18:1679–1687. doi:10.1681/ASN.2006090975
24. Ronzaud C, Loffing J, Gretz N, Schutz G, Berger S (2011) Inducible renal principal cell-specific mineralocorticoid receptor gene inactivation in mice. Am J Physiol Renal Physiol 300:F756–F760. doi:10.1152/ajprenal.00728.2009
25. Rossier BC, Staub O, Hummler E (2013) Genetic dissection of sodium and potassium transport along the aldosterone-sensitive distal nephron: importance in the control of blood pressure and hypertension. FEBS Lett 587:1929–1941. doi:10.1016/j.febslet.2013.05.013
26. Rubera I, Loffing J, Palmer LG, Frindt G, Fowler-Jaeger N, Sauter D, Carroll T, McMahon A, Hummler E, Rossier BC (2003) Collecting duct-specific gene inactivation of alphaENaC in the mouse kidney does not impair sodium and potassium balance. J Clin Invest 112:554–565
27. Rupprecht R, Reul JM, van Steensel B, Spengler D, Soder M, Berning B, Holsboer F, Damm K (1993) Pharmacological and functional characterization of human mineralocorticoid and glucocorticoid receptor ligands. Eur J Pharmacol 247:145–154
28. Schonig K, Schwenk F, Rajewsky K, Bujard H (2002) Stringent doxycycline dependent control of CRE recombinase in vivo. Nucleic Acids Res 30, e134
29. Schulz-Baldes A, Berger S, Grahammer F, Warth R, Goldschmidt I, Peters J, Schutz G, Greger R, Bleich M (2001) Induction of the epithelial Na^+ channel via glucocorticoids in mineralocorticoid receptor knockout mice. Pflugers Arch - Eur J Physiol 443:297–305. doi:10.1007/s004240100694
30. Seibert J, Hysek CM, Penno CA, Schmid Y, Kratschmar DV, Liechti ME, Odermatt A (2014) Acute effects of 3,4-methylenedioxymethamphetamine and methylphenidate on

circulating steroid levels in healthy subjects. Neuroendocrinology 100:17–25. doi:10.1159/000364879

31. Sorensen MV, Grossmann S, Roesinger M, Gresko N, Todkar AP, Barmettler G, Ziegler U, Odermatt A, Loffing-Cueni D, Loffing J (2013) Rapid dephosphorylation of the renal sodium chloride cotransporter in response to oral potassium intake in mice. Kidney Int 83:811–824. doi:10.1038/ki.2013.14
32. Traykova-Brauch M, Schonig K, Greiner O, Miloud T, Jauch A, Bode M, Felsher DW, Glick AB, Kwiatkowski DJ, Bujard H, Horst J, von Knebel DM, Niggli FK, Kriz W, Grone HJ, Koesters R (2008) An efficient and versatile system for acute and chronic modulation of renal tubular function in transgenic mice. Nat Med 14: 979–984. doi:10.1038/nm.1865
33. Zhang W, Xia X, Reisenauer MR, Rieg T, Lang F, Kuhl D, Vallon V, Kone BC (2007) Aldosterone-induced Sgk1 relieves Dot1a-Af9-mediated transcriptional repression of epithelial Na^+ channel alpha. J Clin Invest 117:773–783. doi: 10.1172/JCI29850